

Monitoring Performance Metrics is not Enough to Detect Side-Channel Attacks on Intel SGX

Jiangu Jiang
The University of Hong Kong

Claudio Soriente
NEC Labs Europe

Ghassan Karamé
NEC Labs Europe

Abstract

Side-channel vulnerabilities of Intel SGX is driving the research community towards designing low-overhead detection tools. The ones available to date are grounded on the observation that attacks affect the performance of the victim application (in terms of runtime, enclave interruptions, etc.), so they monitor the potential victim and raise an alarm if the witnessed performance is anomalous.

We show that tools monitoring the performance of an enclave to detect side-channel attacks may not be effective. Our core intuition is that these tools are geared towards an adversary that interferes with the victim’s execution in order to extract the most number of secret bits (e.g., the entire secret) in one or few runs. They cannot, however, detect an adversary that leaks smaller portions of the secret—as small as a single bit—at each execution of the victim. In particular, by minimizing the information leaked at each run, the impact of the attack on the application’s performance is significantly lessened—so that the detection tool notices no attack. By repeating the attack multiple times, and each time leaking a different part of the secret, the adversary can recover the whole secret and remain undetected.

Based on this intuition, we adapt attacks leveraging page-tables and L3 cache so to bypass available detection mechanisms. We show how an attacker can leak the secret key used in an enclave running various cryptographic routines of `libgcrypt`. Beyond cryptographic software, we also show how to leak predictions of enclaves running decision-tree routines of `OpenCV`.

1 Introduction

Intel Software Guard Extensions (SGX) enables applications to execute in isolation from other software on the same platform, including the OS. SGX-enabled processors run applications in so-called *enclaves* and provide them with encrypted runtime memory, encrypted storage, and mechanisms to issue authenticated statements on the enclave

software configuration. Thus, Intel SGX is particularly suited for cloud deployments because it allows to outsource applications to the cloud, with the assurance that the outsourced application runs untampered and its data is not available to any (privileged) software on the same host.

Previous work has shown that Intel SGX has a number side-channels that, coupled with an adversary that controls the OS, allow for effective leakage of enclave secrets [9, 19, 23, 30, 32]. Alongside attacks, the research community has proposed a number of prevention [5, 8, 12, 14, 25] and detection mechanisms [13, 21, 24]—the former having usually much higher overhead compared to the latter. To the best of our knowledge, all detection mechanisms are grounded on the observation that side-channel attacks affect the performance of the victim application (e.g., by increasing the number of enclave interruptions) and, therefore, signal an attack when the witnessed performance is anomalous.

In this paper, we show that such detection tools may not be effective at detecting side-channel attacks on SGX enclaves. We note that existing detection mechanisms are geared towards an adversary that interferes with the victim’s execution in order to extract the most number of secret bits (e.g., the entire secret) in one or few runs. Such an attack strategy has a significant impact on the victim’s performance, effectively allowing detection mechanisms to notice the anomaly and signal the attack. Our core intuition is to leak smaller portions of the secret—as small as a single bit—at each execution of the victim, so as to minimize the impact on its performance and, therefore, remain undetected.

More specifically, we show that an adversary can profile a victim enclave, thereby identifying the precise moment during the victim’s execution when a specific part of the secret can be leaked via a side-channel attack. For example, if the victim runs the popular square-and-multiply algorithm, we show that the attacker can infer the moment when the i -th loop is being executed—i.e., when the i -th secret bit is being processed—and run a side-channel attack at that time to leak the secret bit, while generating almost no relevant events for the detection mechanism. By running the victim multiple times and leaking

a different part of the secret at a time, our technique can recover the whole secret of a victim while remaining undetected.

Based on this intuition, we adapt known attacks leveraging page-tables, L3 cache, and a combination of the two, and show their performance on routines of `libgcrypt` (namely, `mpi_powm` and `mpi_ec_dup_point`) used by popular cryptographic primitives such as ElGamal, RSA, and EdDSA. We also apply our attack strategy on non-cryptographic software and show how to leak predictions of enclaves running decision-tree routines of OpenCV [3]. Our results show that our strategy recovers up to 100% of a secret key used in `libgcrypt` routines, depending on the type of side-channel exploited, and with marginal impact on the victim’s performance (as low as one extra AEX or roughly 40 cache misses per run). In case of a victim using the decision-tree routines of OpenCV to predict handwritten digits of the MNIST data-set [2], our attack strategy can correctly leak around 55% of the predictions (whereas a “standard” side-channel attack, that is easily detected by available tools, reaches 64% of leaked predictions).

We show that an adversary using our attack strategy cannot be detected with existing detection tools such as T-SGX [24], unless one can tolerate a large number of false positives. For example, T-SGX can detect attacks on `mpi_powm` that leverage page-tables, but at the expense of generating false alarms with probability 0.98. Further, we provide evidence that *any* detection tool that monitors the performance of the victim is equally likely to fail. We do so by assuming an “ideal” tool (i.e., one with zero performance penalty) that monitors all of the performance metrics proposed in literature and show that even such a tool may not be able to distinguish a benign execution from one where the victim is under attack.

Our results, therefore, provide strong evidence that observing the performance of an application to detect side-channel attacks on SGX enclaves may not be feasible, and that effective detection mechanisms are yet to be designed.

2 Background & Related Work

In this section, we briefly overview Intel SGX, including side-channel attacks and available defenses.

2.1 Intel Software Guard eXtension (SGX)

Intel SGX is a Trusted Execution Environment available in most recent Intel CPUs. It provides an abstraction called *enclave* that isolates applications and their data from privileged software running on the same host.

Enclave isolation leverages dedicated memory and the hardware performs access control during address translation. However, SGX enclaves share CPU caches with other enclaves and non-enclave processes. Specifically, L1 and L2 caches used by an enclave are shared with processes running on the same core, whereas L3 cache is shared by all program running on the same CPU. Faults and interrupts are

handled by the OS via so-called Asynchronous Enclave eXit (AEX). During an AEX, the execution context of the enclave (e.g., stack and CPU registers) is saved to the so-called State Save Area (SSA) within the enclave memory and control is returned to the OS for interrupt handling.

2.2 Side-channel attacks on SGX

SGX was shown to be vulnerable to cache-based Prime-and-Probe attacks, whereas attacks that exploit shared memory between the victim and the adversary (e.g., Flush+Reload [33] or Flush+Flush [15]) are not applicable—simply because enclaves have dedicated memory.

Brasser et al., [9] show an adapted version of the Prime-and-Probe attack on enclaves where the victim runs uninterruptedly on the same core of the adversary—by using hyper-threading—and cache monitoring uses hardware performance counters to reduce noise in the observations. Schwarz et al., [23] shows an L3 Prime-and-Probe attack that can recover the private RSA key of an enclave by using only 11 traces and leveraging post-processing.

Previous work has also shown that SGX is vulnerable to other side-channels based on, e.g., DRAM [30] or interrupt logic [29].

CacheZoom [19] shows that a malicious OS can actually increase the effectiveness of Prime-and-Probe attacks by running the victim on a dedicated core—to improve spatial resolution—and by interrupting it frequently (via the Advanced Programmable Interrupt Controller)—to improve temporal resolution.

Since the page-table of an enclave is stored in non-protected memory, a privileged attacker can use it as a side-channel. Previous work [25, 32] leaks the memory access pattern—and in turn secret enclave data—by setting the RESERVED bit of all memory pages so to capture each of the enclave page accesses when page-faults occurs.

Previous “Stealthy” Side-Channel Attacks. Previous work proposes side-channel attacks on enclaves that do not cause page-faults—thereby achieving stealthiness despite detection-tools that monitor page-faults. Jo Van et al., [11] monitor the ACCESS bit of the page-table to get the page access sequence of the victim without page-faults. As the ACCESS bit of a page-table is set only the first time the page is accessed (that is subsequent accesses do not modify the bit), the authors of [11] force a TLB shutdown—by interrupting the enclave via inter-process-interrupts—to reset the ACCESS bit. The authors acknowledge that the number of interruptions during their attack is substantially higher than what is to be expected under benign circumstances, and suggest that a detection tool may notice the attack by monitoring enclave interruptions rather than page-faults. Differently, the attack strategy we develop in this paper causes only a few interruptions of the victim and remains undetected.

	Performance Overhead	Detects attacks on						
		L1/L2	L3	page-faults	PTE Monitoring	Our-PF	Our-PFCa	Our-Ca
Varys [21]	~ 15%	✓	×	✓	✓	×	×	×
Déjà Vu [13]	~ 4%	✓	×	✓	✓	×	×	×
T-SGX [24]	~ 108%	×	×	✓	✓	×	×	×
“Ideal” Tool	0%	✓	✓	✓	✓	×	×	×

Table 1: Detection tools for side-channel attacks on Intel SGX. A “✓” (resp. “×”) denotes the fact that the tool can (resp. cannot) detect the attack.

Wang et al., [30] show that enclave interruptions can be minimized if TLB shutdown is achieved by using a sibling hyperthread that probes memory addresses whose TLB entries are conflicted with the ones of the victim enclave. While the attack developed by [30] cannot be detected by monitoring enclave interruptions, it requires the adversary and the victim to run on the same core. As such, the attack is not viable in case of detection tools that enforce core-reservation like Varys [21] or Déjà Vu [13]. Differently, our attack strategy does not require the adversary to run an hyperthread on the core where the victim is running.

2.3 Defenses

Existing defenses can be categorized either as prevention or detection techniques.

Prevention techniques remove leakage by, e.g., preventing untrusted threads from using the victim’s cache [12], rewriting programs to remove secret-dependent page accesses [25] or secret-dependent memory accesses [5], pre-fetching memory [14], or shuffling memory [8]. These approaches usually incur high overhead [5, 14], and sometimes can only prevent specific types of side-channels [12].

Differently, detection techniques have usually lower overhead. To the best of our knowledge, all detection techniques proposed in literature (see Table 1) monitor the execution of the victim application and signal an attack in case of deviations from a “normal” execution. Varys [21] prevents L1/L2 cache-based attacks with core-reservation; at the same time, Varys detects attacks based on page-faults or interrupts by monitoring the number of AEXs so that an alarm is raised if their frequency is too high. We note that Varys is currently part of a commercial product named SCONE and its source-code is not available. Déjà Vu [13] detects attacks based on page-faults or interrupts by monitoring the execution time of the enclave—based on the assumption that AEXs due to faults or interrupts, increase the execution time of a program. Déjà Vu instruments the basic blocks of the enclave code to measure their execution time and an attack is detected if the total time deviates from the one of an execution in a benign environment. An incomplete version of Déjà Vu is available on github¹; we made contact with the authors to obtain the missing code, but they are no longer maintaining the project. T-SGX [24] makes

use of Transactional Synchronization eXtensions (TSX) to detect page-faults. When an interrupt or fault is thrown within a TSX transaction, TSX aborts and executes a user-defined handler. The handler of T-SGX keeps tracks of the number of AEXs and raises an alarm if they reach a given threshold. The source code of T-SGX is available on github².

In Table 1, we also include an “ideal” tool that incurs no performance penalty for the application that uses it, and that monitors all of the performance metrics proposed in literature. We will later show (in Section 5) that even if such a tool were available, it cannot detect an adversary using our attack strategy.

3 Stealthy Side-channel Attacks

3.1 System Model

We assume that the adversary has the victim code available (e.g. the code belongs to a library or an open-source implementation), controls the OS where the enclave is running, and can execute the victim enclave arbitrarily many times.

Such assumptions are similar to the ones found in related work on controlled-channel attacks [19, 30, 32] and capture a realistic cloud scenario where an application is uploaded by its owner to the cloud provider, and part of the application code (e.g., a decryption routine) runs in an enclave. After attestation and secret provisioning by the application owner, the cloud provider can (re-)start the application or trigger the routine running in the enclave arbitrarily many times.

3.2 Main Intuition

As mentioned earlier, detection tools for (known) side-channel attacks leverage the fact that attacks are likely to alter the performance of the victim application. Thus, available detection tools monitor the performance of the potential victim, and signal an attack if the witnessed performance is anomalous.

Our intuition to bypass these tools, is to minimize the effect on the victim’s performance by “spreading” the attack across multiple runs. In particular, we show that an adversary can extract specific portions of the secret, as small as a single bit, at each run of the victim enclave. By minimizing the information leakage at each run, the impact of the attack on the victim’s performance is also lessened—so that the

¹<https://github.com/schuan/dejavu>

²<https://github.com/sslab-gatech/t-sgx>

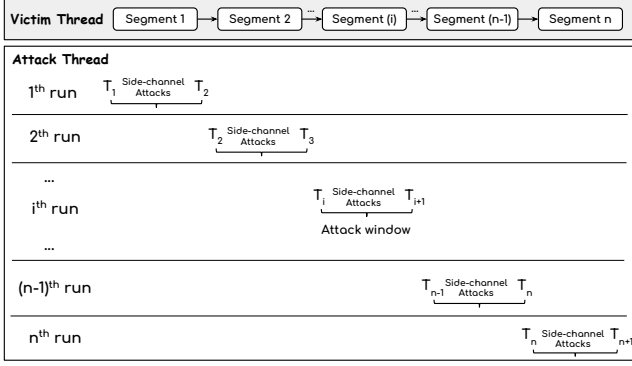


Figure 1: Spreading the attack across multiple runs. Different portions of the secret are leaked at each run.

detection tool notices no anomaly. This strategy is repeated for a number of times—each time leaking a different portion of the secret—to eventually recover the full secret.

In particular, let the enclave secret be $s = s_1, \dots, s_n$, where each s_i could be a single bit or multiple ones. Also, assume the victim code to be split into n segments S_1, \dots, S_n , such that segment S_i processes s_i . As shown in Figure 1, the application is executed n times. During the i -th run, the attack thread launches a side-channel attack while the victim is executing segment S_i , in order to leak s_i . As the attack only runs for a small time-window, the victim’s performance is only marginally affected.

Developing the aforementioned strategy requires the adversary to mount a side-channel attack only during the time-window when the victim is executing code segment S_i . One option would be to precisely control the victim’s execution by using single-stepping frameworks like SGX-Step [28]. Nevertheless, side-stepping the victim generates a large number of page-faults, so a tool that monitors the number of AEXs could easily spot the attack. To remedy this, we take a different approach and design an offline profiling phase to learn the time-interval when the victim is executing a specific code segment S_i . In the following, we detail the offline profiling phase and the design choices we made to minimize errors.

3.3 Application profiling

Let T_i denote the time when the victim starts the execution of code segment S_i . Note that a segment is a logical execution unit and different segments may execute the same code, but on different portions of the secret. For example, in the square-and-multiply routine each segment corresponds to one execution of the main loop and processes a single bit of the secret exponent.

In an ideal scenario, the execution time of each code segment is constant, i.e., $T_{i+1} - T_i = c$. Thus, segment S_i starts at time $T_i = (i-1) \cdot c$, for some constant c . More generally, the execution time of a code segment may depend on the code itself, as well as the portion of the secret it processes. Thus,

```

1 void compute_on_s(char[] p, unsigned int secret) {
2   int tmp = m(p);
3   if ((secret & (1 << i)) != 0) {
4     g(tmp);
5   } else {
6     k(tmp);
7   }
8 }

```

Figure 2: Sample code segment.

we model the execution time of segment S_i as a function $t_i(s_i)$, and set the start time of segment S_i as $T_i = \sum_{j < i} t_j(s_j)$.

As an example, Figure 2 shows a simple code segment with a conditional branch on the i -th bit of variable `secret` and three different function calls (`m`, `g`, and `k`). In case there are no conditional branches nor loops in functions `m`, `g` and `k`, we can use constants to model their execution time as c_m , c_g and c_k , respectively. Thus, $t_i(s_i) = c_m + s_i \cdot c_g + (1 - s_i) \cdot c_k$. In case any of the functions `m`, `g`, `k` has a loop or a conditional branch, we would recursively profile its execution time in a similar fashion.

Once we have the function $t_i(s_i)$ that models the execution of S_i , we assess its values by running S_i multiple times, and by using a different assignment of s_i each time. For example, to measure the execution time of the code in Figure 2, we run the segment twice: once with $s_i = 0$ and once with $s_i = 1$.³ Note that the enumeration of all possible configurations of the part of the secret processed by a code segment is feasible because each segment is likely to process only one or a few secret bits.

Measuring Execution Time. Since SGX cannot execute privileged instructions (e.g., `rdstc`), we cannot directly inject time measurement instructions into code segments. Furthermore, when measuring the execution time of each code segment we cannot interrupt the enclave, as context switches between enclave and non-enclave code incurs extra overhead compared to context switches between regular processes [7, 31]. We, therefore, create a logical clock by means of a timer thread. We inject instructions at the start and end of each segment, to set a binary variable at a memory address `Addr` outside of the enclave memory. A separate timer thread continually gets the system timestamp using `rdstc` and checks the value of the variable at `Addr`. If the variable is set to 1, the timer thread remembers the current timestamp and reset `Addr` to 0. By measuring the time interval between two reads of `Addr` that returned 1, we can infer the time required to run one code segment.

Stabilizing Execution Time. The execution time of arbitrary code on a general-purpose machine is far from deterministic due to the complexity of the host and other software running on it. As in previous work [30], we reduce the noise due to other software on the same host by reserving a core for

³We actually use multiple runs with the same configuration of variables, in order to make our measurements more robust.

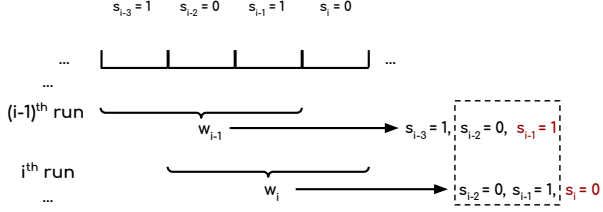


Figure 3: Alignment using a sliding window of size $w = 3$.

the victim enclave. Specifically, we use the `isolcpus` as boot-up option in Ubuntu. As a result, no tasks are assigned to the reserved core, nor it is interrupted for handling I/O. Furthermore, processes can be explicitly assigned to such cores (e.g., using `sched_setaffinity`) and they can be interrupted by inter-processor interrupts. We also note that some detection tools [13, 21] ensure core reservation to avoid side-channel attacks based on L1/L2 caches.

To reduce the noise due to state of the cache when the victim starts, we flush all caches before each execution. Although techniques such as speculative execution may still create differences in the state of the caches across different executions of the enclave, we have empirically verified that each run experiences almost the same amount of cache misses. We also disable dynamic frequency scaling and fix the CPU frequency to stabilize execution time.

By combining core-reservation with cache-flushing and a fixed CPU frequency, we manage to stabilize the execution time of the victim (i.e., within 0.1%).

Improving Attack Accuracy. The accuracy of our technique relies on the correct estimation of T_i —when we start the side-channel attack to learn s_i —and the correct guess of s_i .

Clearly, an error when estimating T_i leads to a misalignment between the attack and the victim that, in turn, leads to unpredictable errors in inferring the secret s_i . An error when inferring s_i may lead to an error in the estimation of T_j for $j > i$ since the start time of segment S_j may depend on the value of s_1, \dots, s_{j-1} .

One possible option (among others) to avoid misalignments between the victim and the attack is to rely on page-faults. In particular, the attacker may invalidate a page that is required by the victim at the start of S_i so that a page-fault is thrown when the victim starts executing that segment. Alternatively, alignment errors may be corrected by attacking multiple consecutive segments at a time by using a sliding window. This basic idea is shown in Figure 3. Let w_i be the window attacking segments S_{i-w+1}, \dots, S_i so to obtain bits s_{i-w+1}, \dots, s_i and, without loss of generality, assume the step of the window to be 1. Then, we compare the guess for bits $s_{i-w+1}, \dots, s_{i-1}$ obtained when attacking window w_i , with the guess for the same bits obtained when attacking window w_{i-1} (i.e., when attacking segments S_{i-w}, \dots, S_{i-1}). If the two bit sequences match, then we assume that window w_i is well aligned and treat the guess for the last bit of the window (i.e.,

```

1 void
2 _gcry_mpi_powm (gcry_mpi_t res,
3                 gcry_mpi_t base, gcry_mpi_t expo, gcry_mpi_t mod)
4 {
5     /* other operations */
6     gcry_mpi_t e = expo;
7     int esec = mpi_is_sec(expo);
8     for (; e != 0; e = (e << 1)) {
9         _gcry_mpih_sqr_n_basecase (xp, rp, rsize);
10        if (esec || (mpi_limb_signed_t)e < 0) {
11            /* mpih_mul (xp, rp, rsize, bp, bsize); */
12            if (bsize < KARATSUBA_THRESHOLD) {
13                _gcry_mpih_mul (xp, rp, rsize, bp, bsize);
14            } else {
15                _gcry_mpih_mul_karatsuba_case (xp, rp, rsize, bp, bsize,
16                                                &karactx);
17            }
18            xsize = rsize + bsize;
19            if (xsize > msize) {
20                _gcry_mpih_divrem(xp + msize, 0, xp, xsize, mp, msize);
21                xsize = msize;
22            }
23            if ((mpi_limb_signed_t)e < 0) {
24                {
25                    tp = rp; rp = xp; xp = tp;
26                    rsize = xsize;
27                }
28            }
29        }
30        /* other operations */
31    }

```

Figure 4: `mpi_powm` used in ElGamal, RSA and DSA.

s_i) as valid; otherwise we assume w_i is not aligned with the victim and discard the guess for s_i .

Note that attacking larger windows may have an impact on the victim’s performance that could allow a detection mechanism to spot the attack. Also, our attack with $w = n$ becomes similar to a “standard” side-channel attack that tries to leak all secret bits at once.

In order to improve the accuracy of our technique, we can also increase the number of times we attack a given segment. That is, we run the victim k times and run the attack on the same segment S_i (or segment window w_i). We therefore obtain several samples for s_i and use heuristics to improve the accuracy of our guess.

4 Leaking secrets of libgcrypt

We now show how to instantiate the strategy described earlier on cryptographic routines `mpi_powm` and `mpi_ec_mul_point` of libgcrypt. The former is the modular exponentiation routine used in a number of cryptographic primitives, including ElGamal, RSA, and DSA; `mpi_ec_mul_point` is the elliptic curve point multiplication routine used by EdDSA. For both victims, we leverage a side-channel based on time as shown in [17, 30], one based on the memory access pattern as shown in [11, 25], and a combination of the two. In the following, we use libgcrypt version 1.7.0. Nevertheless, the side-channels we exploit are present in `mpi_powm` up to version 1.8.6, and in `mpi_ec_mul_point` up to version 1.7.5.

4.1 Side-channels of mpi_powm

Figure 4 shows the code of `mpi_powm`. The routine has two side-channels, one based on time and another based on memory access pattern.

The loop (line 8 ~ 29) consumes one bit of the secret exponent per iteration and executes an extra computation (line 11 ~ 28) if that bit is 1 (line 10). Thus, an adversary can infer the secret bit of the exponent being processed, by inferring the time to complete one loop iteration. Note that if `esec` is 1, then the exponent is stored in secure memory, and the conditional branch is always executed to eliminate side-channels. However, if `xvalue` is provided as input by the user (e.g., when the key-pair is generated from a passphrase), then `libgcrypt` does not store the exponent in secure memory so that side-channels are not eliminated.

Alternatively, the secret bit of the exponent can be leaked by monitoring access to memory pages that store the code required by the `if`-branch of the routine. Let `A`, `B`, `C` be the addresses of `mpi_powm`, `mpi_mpih_sqr_n_basecase` and `mpihelp_mul`, respectively. One iteration of the loop where the exponent bit is 1, shows a memory access sequence like `ABCAC|AB`, whereas if the exponent bit is 0, the observed memory access sequence is like `ABC|AB`. In these examples, memory accesses after `|` belong to the next iteration of the loop. Also, note that `mpi_mpih_sqr_n_basecase` calls `mpihelp_mul`, so there will always be an access to address `C` after `B`. One could infer the memory access sequence either by observing page-faults or cache accesses.

4.2 Profiling of mpi_powm

In order to profile `mpi_powm`, we define each iteration of the main loop as one segment. Let s_i be the i -th exponent bit consumed in segment S_i . One iteration of the loop in `mpi_powm` computes on `xp`, `rp` and s_i . We found no branches nor loops in `mpih_sqr_n_basecase`, so its runtime is constant and we denote it as c_{base} . Thus, runtime of S_i with $s_i = 0$ is simply c_{base} . If $s_i = 1$, the code executed (lines 11 ~ 28) has two branches. The first one is a conditional branch that, depending on the value of `bsize`, may run either `mpihelp_mul` or `mpihelp_mul_karatsuba_case`. We found that both paths take the same time so we model this time as a constant $c_{mpihelp}$. The second branch depends on `xsize` and `msize`. However, we found that the time taken to run `mpihelp_divrem` is negligible, so we just ignore it. In a nutshell, the time to run segment S_i is $t_i(s) = c_{base} + s_i \cdot c_{mpihelp}$ and $T_i = (i-1) \cdot c_{base} + \sum_{j < i} s_j \cdot c_{mpihelp}$.

4.3 Page-faults

We start by describing an instantiation of our attack strategy that only uses page-faults and that leverages the timing side-channel of the victim; we denote this attack variant as Our-PF.

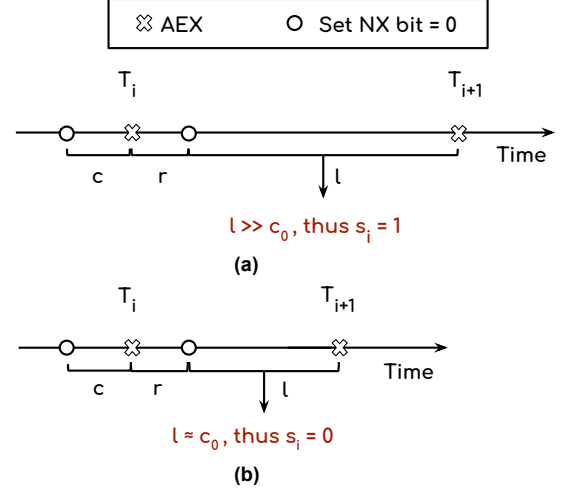


Figure 5: Workflow of Our-PF when secret bit s_i is 1 (a) or 0 (b).

More specifically, for $i = 1, \dots, n$, we start the victim enclave running `mpi_powm`, and use a single page-fault to stop it at the beginning of segment S_i . Next, we resume the victim and measure—again, using one page-fault—the time it takes to complete that segment, in order to learn the secret bit s_i .

Figure 5 shows how the Our-PF attack strategy works. Assume the time it takes to run one iteration of the loop with exponent bit 0 and 1 is c_0 and c_1 (with $c_0 < c_1$), respectively. We start the victim and set the NX bit of the page containing `mpih_sqr_n_basecase`, right before time T_i (i.e., at $T_i - c$, for some small constant c). As a result, the victim stops and throws a page-fault at the beginning of segment S_i —i.e., at the beginning of the i -th iteration of the loop. At this time, we resume the victim enclave, and set again the bit NX of the page of `mpih_sqr_n_basecase`. Therefore, the next page-fault will be thrown when the victim moves to the next segment. Hence, the time between the two page-faults is compared against c_0 and c_1 , to decide the value of bit s_i . Once we learn s_i , we compute T_{i+1} accordingly and move on to attack the next segment. This process is repeated for $i = 1, \dots, n$ in order to recover the whole secret. In practice, we also make sure that the NX bit is not set while the victim is running `mpih_sqr_n_basecase`. We do so by ensuring that the bit is set r ticks after the page-fault, where r is the number of ticks required to run `mpih_sqr_n_basecase`.

4.4 Page-fault and Cache

We now describe another attack variant that leverages both page-faults and cache misses, that we refer to as Our-PFCa. As Our-PFCa only leverages a side-channel based on memory access pattern, it could be used on routines that have no side-channel based on time.

Similar to Our-PF, we use one page-fault to stop the enclave at the beginning of each segment. Then, we use a

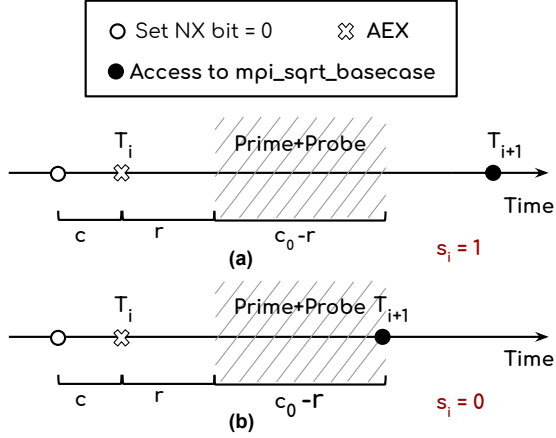


Figure 6: Workflow of Our-PFCa when secret bit s_i is 1 (a) or 0 (b).

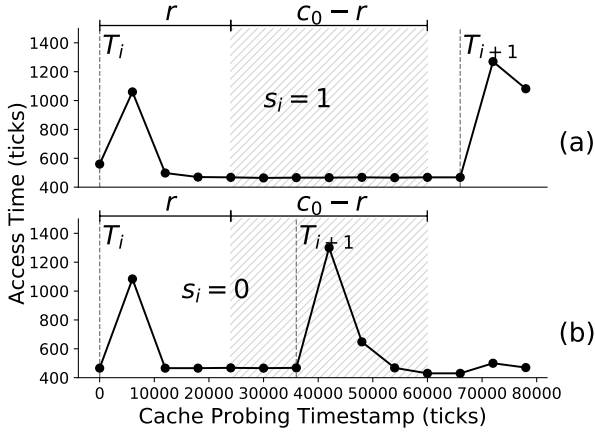


Figure 7: L3 probing pattern of mpi_powm using Our-PFCa.

Prime-and-Probe attack on L3 cache to infer the secret bit processed during the execution of that segment. We use L3 since most detection tools prevent L1/L2 attacks by ensuring that no untrusted thread runs on the same core of the thread being monitored (see Table 1).

The workflow of Our-PFCa is shown in Figure 6. Let c_0 and c_1 (with $c_0 < c_1$) be the time it takes to run one loop of mpi_powm with secret bit 0 and 1, respectively. We stop the enclave at $T_i - c$ by making the page of mpih_sqr_n_basecase unavailable at that time; next, we resume the victim and wait for r clock ticks to make sure that computation on mpih_sqr_n_basecase is over. Now, the goal is to measure whether the next call to mpih_sqr_n_basecase happens after time $c_0 - r$ or $c_1 - r$. To do so, we start a Prime-and-Probe attack on the address of mpih_sqr_n_basecase, for a period of $c_0 - r$. We construct the eviction set of the Prime-and-Probe using techniques from previous research [18]. Figure 7 shows the time to access the target cache set when the secret bit is 1 (a) or 0 (b). Here, it is clear that the victim has accessed the cache line of mpih_sqr_n_basecase if the

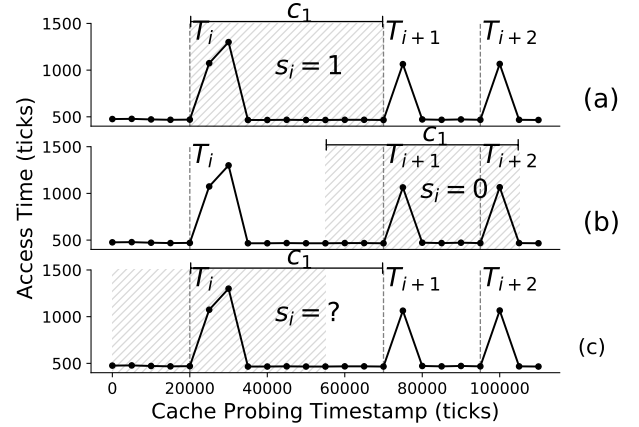


Figure 8: L3 probing pattern of mpi_powm using Our-Ca.

access time of the attacker to the eviction set is larger than 1000 ticks. The first peak in each figure denotes the start of the i -th iteration, while the shaded area denotes the interval of $c_0 - r$ ticks during which we run the Prime-and-Probe attack. Note that if s_i is 1 (Fig. 7a) we do not witness any access to mpih_sqr_n_basecase while running the Prime-and-Probe attack. In case s_i is 0 (Fig. 7b) we witness access to mpih_sqr_n_basecase as the routine moves to the next iteration of the loop. Once we learn s_i , we compute T_{i+1} accordingly, and move on to attack the next segment.

4.5 Cache-only

The attack strategies above use page-faults to temporally align the victim and attack threads. We now show how to run cache-only attacks on the victim enclave. In the sequel, we refer to this strategy as Our-Ca.

Note that, using only cache to leak a specific portion of the victim's secret may be difficult because the adversary thread may not be aligned with the one of the victim; nevertheless, Our-Ca is particularly effective with detection tools that monitor enclave exits (AEXs) [22, 24] as it enables the leakage of the secret without interrupting the victim at all.

Our-Ca works by starting a Prime-and-Probe attack on the address of mpih_sqr_n_basecase right before T_i and for c_1 ticks—the number ticks required to complete the loop iteration when the secret bit is 1. If the attack thread experiences a peak in the time to access the target cache set, followed by a sufficient number of lows, we conclude that $s_i = 1$, whereas if the attack thread experiences two close peaks, we conclude that $s_i = 0$.

A considerable challenge when using Our-Ca lies in the fact that small errors when estimating T_i leads to unpredictable cache patterns. This is shown in Figure 8. In Figure 8(a), the attack starts at the right time and the witnessed cache pattern does indeed support a correct guess of s_i . Differently, in Figure 8(b) the attack starts late and

```

1 void
2 _gcry_mpi_ec_mul_point (mpi_point_t result,
3                        gcry_mpi_t scalar, mpi_point_t point,
4                        mpi_ec_t ctx)
5 {
6     /* Other operations */
7     if (mpi_is_secure (scalar))
8     {
9         /* Oblivious Implementation */
10    } else {
11        for (j=nbits-1; j >= 0; j--) {
12            _gcry_mpi_ec_dup_point (result, result, ctx);
13            if (mpi_test_bit (scalar, j)) {
14                _gcry_mpi_ec_add_points (result, result, point, ctx);
15            }
16        }
17    }
18    /* Other operations */
19 }

```

Figure 9: `mpi_ec_mul_point` used in EdDSA.

the adversary (mistakenly) estimates s_i to be 0. Finally, in Figure 8(c), the attack starts early, preventing the adversary from estimating the value of the secret bit.

We correct alignment errors between adversary and victim by using a sliding window technique as explained in Section 3. That is, when attacking window w_i (i.e., segments S_{i-w+1}, \dots, S_i) we start the Prime-and-Probe attack right before T_{i-w+1} and we run it for $w \cdot c_1$ ticks—i.e. until the end of segment S_i . Next, we consider the estimate of s_i as valid only if the estimate of $s_{i-w+1}, \dots, s_{i-1}$ matches the estimate of the same bits when attacking window w_{i-1} . Finally, we also repeat the attack on the same window a number $k \geq 1$ of times in order to obtain multiple guesses for the same bit and use an heuristic to infer its actual value.

4.6 Attacks on `mpi_ec_mul_point`

We now briefly discuss how to adapt our attack strategy to the `mpi_ec_mul_point` routine of `libgcrypt` used in EdDSA. For each signature, this subroutine is used to compute scalar multiplication with a nonce that, if leaked, allows the recovery of the signing key. Note that our attack extracts one secret bit for each execution of the victim; hence, if the victim picks a fresh nonce at each execution, two bits extracted by our attack would be completely uncorrelated. Nevertheless, EdDSA is deterministic [27] and the nonce is computed as function of the message to be signed and the signing key. Hence, by feeding a fixed message to the signing routine we ensure that the nonce is always the same and can extract one of its bits at each execution.

Figure 9 shows the code of `mpi_ec_mul_point`. Note that the same routine is used to process both the nonce and the signing key (referred to as `scalar` in both cases). The leakage-free code (line 7 ~ 10) is used when processing the signing key, whereas the `else`-branch is taken to process the nonce. In the latter case, a secret-dependent branch (line 13) can be abused to leak one bit of the (secret) nonce. Once the nonce and the corresponding signature are available, the

signing key can be computed.

Profiling `mpi_ec_mul_point`. Let segment S_i be the i -th iteration of the loop. We found that there are no conditional loops nor branches in `gcry_mpi_ec_dup_point` so we model its execution time with constant c_{base} . In case the bit of `scalar` being processed is 1, the routine calls another constant-time function called `mpi_ec_add_point` and we model its execution time with constant c_{add} . Therefore, the running time of the i -th loop iteration is $t_i(s) = c_{base} + s_i \cdot c_{add}$, and the start time of the i -th segment is $T_i = (i-1) \cdot c_{base} + \sum_{j<i} s_j \cdot c_{add}$.

In practice, we must also accommodate for the first iteration of the loop that takes the `if`-branch; this iteration must fetch `mpi_ec_add_point` and its callees from the main memory and incurs in a time increase that we model with c_{miss} . Thus the start time for the i -th segment becomes $T_i = (i-1) \cdot t_{base} + \sum_{j<i} s_j \cdot c_{add} + (\sum_{j=1}^{i-1} s_j \bmod 2) \cdot t_{cache_miss}$. This extra time for the first loop that processes a 1 bit does not show in `mpi_powm`, as the secret-dependent call to `mpi_sqrt_n_basecase` is also called in other function before `mpi_powm`.

When attacking `mpi_ec_mul_point` we use the page containing `mpi_ec_dup_point` to stop the enclave at the beginning of the target segment. Further, we target `mpi_ec_dup_point` when launching the Prime-and-Probe attack.

5 Results for `libgcrypt`

We instantiated the relevant routines of `libgcrypt` 1.7.0 in SGX, by using Panoply [26] to delegate system calls out of enclave. Our experiments were carried out with Ubuntu 18.04 on an Intel E3-1280 with 4 physical cores and 32GB RAM.

To assess the effectiveness of our adapted attacks despite existing detection tools, we compiled and run the two cryptographic routines using T-SGX with some engineering efforts. The abort handler in its code simply recomputes after aborts, and we modified the handler to forward page-fault handling to the system.

As the other two detection tools available in literature are not open-source—Varys is part of a commercial product and Déjà Vu is no longer maintained—we also evaluate the effectiveness of our strategy on enclaves equipped with an “ideal” tool. We assume the latter to require no code instrumentation (hence, “ideal” in terms of performance overhead), to monitor all of the performance metrics proposed in literature (i.e., number of AEX, cache misses, and execution time), and to raise an alarm if the witnessed performance is anomalous. We note that cache misses are typically monitored via performance counters—a feature that is not currently available for SGX enclaves. Nevertheless, previous work has shown that (non-SGX) applications could use cache-misses to detect cache-based attacks [10]; hence, we include the

number of cache misses among the performance metrics that are monitored by the ideal tool to emulate the possibility that it becomes available to future SGX applications.

5.1 Profiling Accuracy

We start by measuring the execution time of one loop of the victim routines—recall that a loop of `mpi_powm` and `mpi_ec_mul_point` is a code segment as defined in Section 3. We do so by running each loop 100 times with secret bit 0 and another 100 times with secret bit 1.

Our results show that, in case of using the ideal tool, a “0-loop” of `mpi_powm` takes on average 46.4k clock ticks ($\sigma = 493.6$), while a “1-loop” takes on average 92.9k clock ticks ($\sigma = 122.2$). When instrumented with T-SGX, `mpi_powm` takes slightly longer: 48.3k clock ticks ($\sigma = 530.1$) for a 0-loop and 103.2k clock ticks ($\sigma = 251.3$) for a 1-loop.

Routine `mpi_ec_mul_point` with the ideal tool, takes on average 15.4k clock ticks ($\sigma = 378.1$) for a 0-loop, and 39.2k clock ticks ($\sigma = 284.9$) for a 1-loop. When instrumented with T-SGX, `mpi_ec_mul_point` nearly double its computation time: it takes 38.8k clock ticks ($\sigma = 631.3$) and 92.0k clock ticks ($\sigma = 376.1$) for 0-loop and 1-loop, respectively.

Once we have the running times for 0-loop and 1-loop iterations, we validate the accuracy of our profiling technique by checking whether we can stop the enclave at the start of each loop. To do so, we fix a random 256 bit secret and we execute the enclave 256 times, each time stopping it (by leveraging a page-fault) at time $T_i - c$ (with $i = 1, \dots, 256$ and $c = 5,000$ clock ticks).⁴ In order to learn the ground truth, we inject a counter into the code to keep track of the number of loop iterations thus far. This experiment is repeated 20 times and we report the results in Table 2.

Our evaluation shows that stopping at a specific code segment an enclave running `mpi_powm` with the ideal tool is more accurate (93.17%) than achieving the same if the enclave runs the routine instrumented with T-SGX (85.08%). This is because we may lose synchrony with the victim as T-SGX restarts a transaction. We observe the same behavior for `mpi_ec_mul_point`: 81.74% for the version using the ideal tool and 68.19% for the version instrumented with T-SGX. A comparison between `mpi_powm` and `mpi_ec_mul_point` shows lower accuracy for the latter. This is because one loop of `mpi_ec_mul_point` takes less time to complete compared to a loop of `mpi_powm`—therefore, it is harder to hit the start of a specific loop iteration.

5.2 Attack Accuracy

We evaluate the accuracy of the three adapted attack variants in recovering secret bits. To do so, we fix a random 256 bit secret and, for $i = 1, \dots, 256$, we recover the secret bit s_i by

⁴Note that we can correctly estimate any T_i because we know the value of the secret bits.

	Accuracy
<code>mpi_powm</code> (w/ ideal tool)	93.17% ($\sigma = 5.49\%$)
<code>mpi_powm</code> (w/ T-SGX)	85.08% ($\sigma = 8.90\%$)
<code>mpi_ec_mul_point</code> (w/ ideal tool)	81.74% ($\sigma = 4.52\%$)
<code>mpi_ec_mul_point</code> (w/ T-SGX)	68.19% ($\sigma = 1.40\%$)

Table 2: Accuracy when stopping the victim enclave at the beginning of a specific code segment.

attacking the corresponding code segment 9 times (i.e., for 9 times we run the enclave and launch the side-channel attack from T_i until T_{i+1}). Given the 9 samples, we determine the secret bit based on majority voting. We repeat the experiment 10 times and show the average accuracy and standard deviation in the column “Attack Accuracy” in Table 3 and Table 4 for `mpi_powm` and `mpi_ec_mul_point`, respectively. For comparison purposes, we also report the accuracy of “standard” side-channel attacks using either page-faults [30] or L3 cache [17, 30]. A standard attack refers to an attack that runs throughout the whole execution of the victim in order to recover the largest number of secrets bits in one execution. In case of standard attacks we also repeat the attack 9 times and use majority voting to decide the value of each secret bit. Note that, in case of routines instrumented with T-SGX, a standard page-faults attack does not work as the detection tools raises an alarm shortly after the attack starts.

Table 3 and Table 4 show that our attack strategy can recover between 60% and 100% of the enclave secret, depending on (i) the type of side-channel exploited, (ii) the detection tool used by the victim (either T-SGX or an ideal tool), and (iii) the number of consecutive code segments attacked per run. For example, we can extract around 80% of the secret using Our-PF and up to 100% of the secret using Our-Ca. Our experiments also show that attack accuracy decreases when the victim is instrumented with T-SGX: this is likely due to the noise introduced by T-SGX when restarting transactions that abort before completion.

Comparing the accuracy of attacks on `mpi_powm` with the accuracy when attacking `mpi_ec_mul_point`, we note that Our-PF performs better on `mpi_powm` and this is because the time difference between a 1-loop and a 0-loop in that routine is sharper than the time difference of the loops in `mpi_ec_mul_point`. Nevertheless, attack variants that use cache are more accurate on `mpi_ec_mul_point` as the cache side-channel is more noisy when attacking `mpi_powm`. Furthermore, cache-only attack with larger windows (e.g., $w=9$) provide very good results.

We also assess the impact of the number of samples k we obtain for each secret bit on the attack accuracy. As shown in Figure 10, increasing k improves accuracy that, however, plateaus around $k=9$ for most of the attack variants.

Finally, we assess the impact on accuracy when relying on a sliding window to reduce alignment errors in cache-only attacks. Recall that attacking a single segment at a time by

		Detection Tool	Attack Accuracy	AEX	L3 Cache-misses	Time (ms)
Our attacks	Our-PF	ideal	85.5% ($\sigma = 7.9\%$)	3.04 ($\sigma = 0.20$)	125.91 ($\sigma = 82.72$)	5.67 ($\sigma = 0.031$)
	Our-PFCa		69.8% ($\sigma = 6.1\%$)	2.70 ($\sigma = 0.53$)	175.05 ($\sigma = 135.05$)	5.64 ($\sigma = 0.014$)
	Our-Ca ($w=3$)		76.3% ($\sigma = 10.1\%$)	1.32 ($\sigma = 0.46$)	164.05 ($\sigma = 47.06$)	5.62 ($\sigma = 0.010$)
	Our-Ca ($w=5$)		89.14% ($\sigma = 13.54\%$)	1.39 ($\sigma = 0.48$)	218.81 ($\sigma = 23.67$)	5.62 ($\sigma = 0.0099$)
	Our-Ca ($w=9$)		99.7% ($\sigma = 0.5\%$)	1.30 ($\sigma = 0.46$)	275.76 ($\sigma = 38.02$)	5.62 ($\sigma = 0.011$)
	Our-PF	T-SGX	80.73% ($\sigma = 9.66\%$)	3.49 ($\sigma = 0.50$)	149.04 ($\sigma = 87.56$)	5.71 ($\sigma = 0.04$)
	Our-PFCa		61.2% ($\sigma = 8.8\%$)	2.47 ($\sigma = 0.68$)	180.10 ($\sigma = 106.30$)	5.71 ($\sigma = 0.02$)
	Our-Ca ($w=3$)		76.10% ($\sigma = 10.52\%$)	1.20 ($\sigma = 0.41$)	237.06 ($\sigma = 115.11$)	5.66 ($\sigma = 0.06$)
	Our-Ca ($w=5$)		86.42% ($\sigma = 14.32\%$)	1.23 ($\sigma = 0.43$)	284.94 ($\sigma = 69.83$)	5.68 ($\sigma = 0.05$)
	Our-Ca ($w=9$)		100%	1.21 ($\sigma = 0.42$)	388.20 ($\sigma = 87.73$)	5.67 ($\sigma = 0.04$)
Standard attacks	Page-faults attack	ideal	97.9% ($\sigma = 3.2\%$)	831.97 ($\sigma = 99.69$)	124.16 ($\sigma = 21.78$)	11.50 ($\sigma = 0.758$)
	Cache attack		89.5% ($\sigma = 4.3\%$)	1.67 ($\sigma = 0.71$)	2112.86 ($\sigma = 82.10$)	5.68 ($\sigma = 0.0078$)
	Page-faults attack	T-SGX	0%	N/A	N/A	N/A
	Cache attack		84.4% ($\sigma = 9.6\%$)	1.31 ($\sigma = 0.45$)	3697.68 ($\sigma = 817.95$)	5.81 ($\sigma = 0.013$)
No attack	mpi_powm	ideal		2.441 ($\sigma = 1.93$)	123.27 ($\sigma = 82.91$)	5.63 ($\sigma = 0.017$)
	mpi_powm (w/ GCC)			14.44 ($\sigma = 10.97$)	495.0 ($\sigma = 290.11$)	5.78 ($\sigma = 0.09$)
	mpi_powm (w/ Redis)			1.48 ($\sigma = 0.70$)	6007.21 ($\sigma = 510.83$)	6.05 ($\sigma = 0.48$)
	mpi_powm	T-SGX		2.30 ($\sigma = 0.69$)	242.74 ($\sigma = 305.69$)	5.66 ($\sigma = 0.02$)
	mpi_powm (w/ GCC)			23.55 ($\sigma = 2.48$)	394.14 ($\sigma = 549.7$)	5.71 ($\sigma = 0.60$)
	mpi_powm (w/ Redis)			1.47 ($\sigma = 0.75$)	16256.47 ($\sigma = 5843.78$)	6.12 ($\sigma = 0.25$)

Table 3: Accuracy and performance metrics for mpi_powm.

		Detection Tool	Attack Accuracy	AEX	L3 Cache-misses	Time (ms)
Our attacks	Our-PF	ideal	69.6% ($\sigma = 3.3\%$)	3.01 ($\sigma = 0.12$)	98.16 ($\sigma = 14.12$)	6.31 ($\sigma = 0.012$)
	Our-PFCa		64.4% ($\sigma = 2.7\%$)	2.33 ($\sigma = 0.47$)	155.94 ($\sigma = 112.04$)	6.30 ($\sigma = 0.010$)
	Our-Ca ($w=3$)		86.4% ($\sigma = 12.91\%$)	1.60 ($\sigma = 0.49$)	186.43 ($\sigma = 16.99$)	6.29 ($\sigma = 0.012$)
	Our-Ca ($w=5$)		100%	1.50 ($\sigma = 0.49$)	201.41 ($\sigma = 22.22$)	6.29 ($\sigma = 0.011$)
	Our-Ca ($w=9$)		100%	1.50 ($\sigma = 0.50$)	249.38 ($\sigma = 22.75$)	6.29 ($\sigma = 0.012$)
	Our-PF	T-SGX	59.4% ($\sigma = 4.4\%$)	3.07 ($\sigma = 0.31$)	151.47 ($\sigma = 206.39$)	14.02 ($\sigma = 0.48$)
	Our-PFCa		57.3% ($\sigma = 5.5\%$)	3.05 ($\sigma = 0.75$)	187.52 ($\sigma = 122.16$)	13.95 ($\sigma = 0.40$)
	Our-Ca ($w=3$)		61.44% ($\sigma = 14.1\%$)	3.33 ($\sigma = 0.48$)	268.35 ($\sigma = 562.07$)	13.45 ($\sigma = 0.26$)
	Our-Ca ($w=5$)		75.91% ($\sigma = 10.1\%$)	3.39 ($\sigma = 0.49$)	257.92 ($\sigma = 448.48$)	13.70 ($\sigma = 0.32$)
	Our-Ca ($w=9$)		100%	3.37 ($\sigma = 0.49$)	305.34 ($\sigma = 524.03$)	13.36 ($\sigma = 0.24$)
Standard attacks	Page-faults attack	ideal	99.6% ($\sigma = 0.22\%$)	499.28 ($\sigma = 96.31$)	98.80 ($\sigma = 21.09$)	10.19 ($\sigma = 0.76$)
	Cache attack		96.8% ($\sigma = 5.0\%$)	1.47 ($\sigma = 0.50$)	9684.87 ($\sigma = 701.08$)	6.46 ($\sigma = 0.011$)
	Page-faults attack	T-SGX	0%	N/A	N/A	N/A
	Cache attack		96.6% ($\sigma = 3.8\%$)	3.44 ($\sigma = 0.51$)	15730.48 ($\sigma = 4363.18$)	14.17 ($\sigma = 0.19$)
No attacks	mpi_ec_mul_points	ideal		2.71 ($\sigma = 2.28$)	106.23 ($\sigma = 60.79$)	6.29 ($\sigma = 0.012$)
	mpi_ec_mul_points (w/ GCC)			23.21 ($\sigma = 27.83$)	1246.31 ($\sigma = 1331.89$)	6.30 ($\sigma = 0.02$)
	mpi_ec_mul_points (w/ Redis)			1.61 ($\sigma = 0.83$)	6092.45 ($\sigma = 1043.90$)	7.21 ($\sigma = 1.02$)
	mpi_ec_mul_points	T-SGX		3.64 ($\sigma = 1.24$)	200.36 ($\sigma = 538.88$)	13.31 ($\sigma = 0.29$)
	mpi_ec_mul_points (w/ GCC)			24.37 ($\sigma = 3.36$)	817.54 ($\sigma = 1331.89$)	13.67 ($\sigma = 0.50$)
	mpi_ec_mul_points (w/ Redis)			4.39 ($\sigma = 1.12$)	84941.38 ($\sigma = 25664.85$)	17.69 ($\sigma = 1.17$)

Table 4: Accuracy and performance metrics for mpi_ec_mul_point.

only using cache side-channels may lead to poor results due to the difficulty of aligning the victim and attack threads (see Section 3). In our experiments, a cache-only attack on one segment at a time resulted in an average accuracy over 20 runs of 46.64% ($\sigma = 3.84\%$) for mpi_powm with the ideal tool; the accuracy for the version instrumented with T-SGX was 48.44% ($\sigma = 3.4\%$). The same experiment when attacking mpi_ec_mul_point showed an average accuracy of 51.64% ($\sigma = 1.98\%$); the accuracy for the version instrumented with T-SGX was 50.3% ($\sigma = 3.7\%$). By using the sliding window technique described in Section 3, we improve accuracy as shown in Figure 11. In particular, a window of size $w = 9$ allows to recover the full secret when attacking mpi_powm, whereas the same result can be achieved with a window of size $w = 5$ for mpi_ec_mul_point. This is because, the cache side-channel is less noisy in mpi_ec_mul_point, as explained before.

5.3 Effectiveness Against Detection Tools

We now assess the effectiveness of T-SGX and the ideal tool described above in detecting our attack strategy. Recall that T-SGX monitors the number of AEXs whereas the ideal tool monitors all of the performance metrics proposed in literature, namely number of AEXs, execution time, and cache misses.

We collect the aforementioned performance metrics, when the victim is under attack, as well as when the victim is running in a benign environment either (i) alone or (ii) while another process is running on the same machine. For the latter, we used either Redis—a key-value store—and we mimic a realistic workload as in [4], or GCC while building a large project. Finally, we record the required performance metrics while attacking the victim with standard side-channel attacks.

On the one hand, reported figures on routines instrumented with T-SGX provide us with evidence of the effectiveness

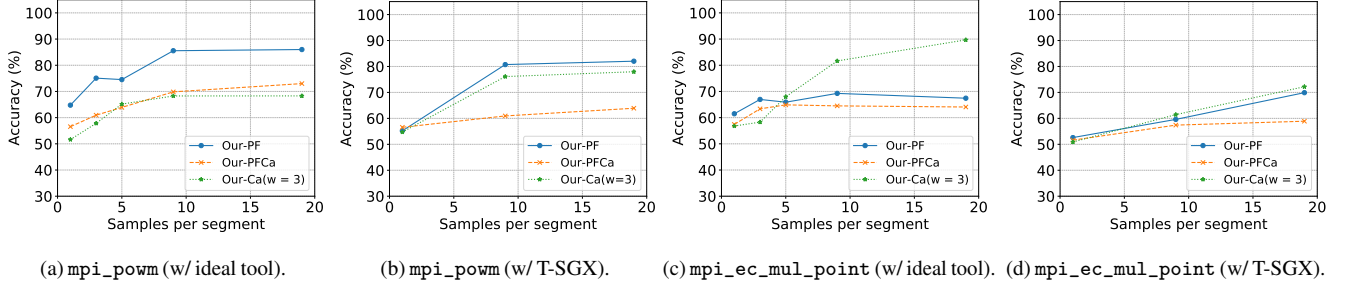


Figure 10: Accuracy versus number of samples per segment.

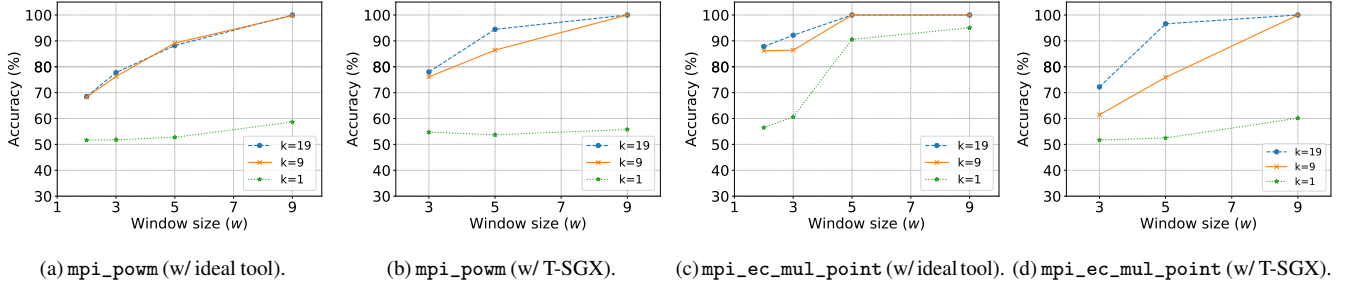


Figure 11: Accuracy versus window-size for Our-Ca. Label “k” refers to the number of samples per segment.

of our adapted attacks when the victim is equipped with existing tools. On the other hand, results of the experiments with an ideal tool allow us to reason about effectiveness of our adapted attacks with respect to any tool that monitors the performance of the potential victim. For each scenario, we run the victim 1,000 times and report the average and standard deviation in Table 3 and Table 4.

For each of the considered scenarios and for different values of detection thresholds, we also measure *recall* (ratio of true positives over all positive cases) and *specificity* (ratio of true negatives over all negative cases). The recall metric is used to measure security: a perfect tool should have recall equal to one, and any smaller value means that the tool is not detecting some attacks. Specificity measures usability: a perfect tool should have specificity equal to one, and any smaller value means that the tool is raising some false alarms. In a real deployment, detection thresholds should be set so that both recall and specificity are as close as possible to one. In the following, we show that, for both T-SGX and the ideal tool, high specificity and high recall cannot be achieved at the same time—which shows that such tools cannot detect an adversary that use our attack strategy.

Detection with T-SGX. In this set of experiments, we run the victim instrumented with T-SGX along with GCC to mimic a realistic multi-threaded workload. We vary the threshold number of AEXs before T-SGX raises an alarm, and measure specificity and recall for each threshold.

Figure 12a shows results for `mpi_powm`. No threshold in the range we consider ($2 \leq t \leq 10$) provides specificity greater than 0.03—hence, one should set the threshold to a value

much larger than 10 to avoid false alarms. At the same time, all of the attack variants exhibit zero recall for $t \geq 5$. Figure 12b shows very similar results for `mpi_ec_mul_point`. Specificity does not increase above 0.03 for $t \leq 10$ and all of the attack variants reach zero recall for $t \geq 6$.

Detection with the ideal tool. In case of the ideal tool, we consider detection based on both the number of AEXs and the number of cache misses. For each scenario, we run the victim either along with GCC—to mimic a multi-threaded workload—or along with Redis—as an exemplary application to mimic a memory-intensive workload. Further, we vary the detection threshold—either the one of number of AEXs or the one of number of cache misses—and measure specificity and recall for each threshold.

Figure 13a and Figure 13b show results when the tool is monitoring AEXs and the victims are `mpi_powm` or `mpi_ec_mul_point`, respectively. No threshold in the range we consider ($2 \leq t \leq 10$) provides specificity greater than 0.37 in case of `mpi_powm` and 0.55 in case of `mpi_ec_mul_point`. At the same time, all of the attack variants go undetected (recall is 0) if $t \geq 5$ for both victims.

Figure 13c and Figure 13d depict our results when the tool is monitoring cache misses and the victims are `mpi_powm` or `mpi_ec_mul_point`, respectively. For both victims, specificity is 0 for thresholds up to 800; therefore, the tool raises a false alarm at every run and one should set much higher thresholds to avoid false alarms. However, all of the attacks go undetected if $t \geq 800$ for `mpi_powm` or $t \geq 600$ for `mpi_ec_mul_point`.

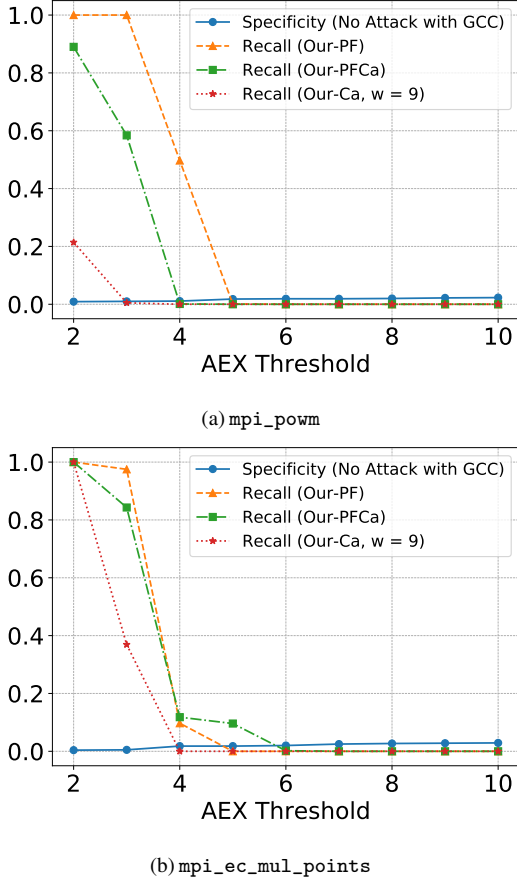


Figure 12: Specificity and recall of detection based on T-SGX when GCC is running on the same host.

Detection by monitoring execution time. A detection tool may monitor the execution time to decide whether the application is under attack. This is for example the case of Déjà Vu [13]. Results from Table 3 and Table 4 show that standard page-fault attacks almost double the execution time and would be likely detected by tools such as Déjà Vu. Differently, our attacks cause minimal increase of the victim’s execution time (below 2%); as such, it is challenging for Déjà Vu or similar tools to detect them.⁵

6 The Case of OpenCV

We now adapt our attack strategy to known side-channels of decision-tree routines [20] in order to attack the decision-tree routine of OpenCV [3], a well-known computer vision library. Similar to previous work [1], we use the MNIST [2] data-set

⁵Note that for a 256 bit secret, attacking a single segment takes roughly 6 ms (see for example the running time of `mpi_powm` in Table 3). In this case, recovering the full secret requires approximately 1536 ms. In case the adversary attacks each segment $k=9$ times to obtain higher accuracy, the total attack time increases to roughly 13.8 seconds.

and assume an application consisting of an enclaved execution of OpenCV’s decision-trees to detect handwritten digits.

Figure 14 shows the code of OpenCV’s decision-tree traversal function `DTreesImpl::predictTrees`. This function traverses the tree and, depending on the input image, accesses different nodes (`nodes[nidx]`), resulting in different page accesses. We use page-faults to infer the pattern of page accesses and leak the prediction output. To capture the access pattern of different input images, we rely on an offline analysis of the routine and observe memory page access patterns of different nodes `[nidx]` for prediction output. These memory pages are set as fault during runtime, to infer the prediction output. To reduce the number of page-faults during attacks, we eliminate memory page accesses that cannot identify two unique secrets. For example, if prediction “1” and “2” produces access sequence ACD and ACE, respectively, then we use only page A, D and E for inferring the prediction.

We ported OpenCV’s decision-tree library (the i.e., `core` and `ml` modules) to SGX by forwarding system calls (e.g., `fread` and `fopen`) outside enclave. For training the decision-tree, we use 60,000 samples from the MNIST data set. During the inference phase, the trained decision-tree model is first loaded into the enclave and then used to recognize 100 input images at a time from a set of 10,000 test images. The execution time of image recognition is almost independent of the input image, as the tree is almost balanced. Therefore, we can model the execution time as $T_i = T_i + c$, where c is a constant value. In our experiments, we found out that c is roughly 9.7k clock ticks ($\sigma=975.3$).

Profiling and Attack Accuracy. In our experiments, we were able to stop the enclave at the time of the i -th invocation of `DTreesImpl::predictTrees` around 8 out of 10 times (84.8% ($\sigma = 7.85\%$)). The corresponding attack accuracy is reported in Table 5—our attack that only leverages page-faults (Our-PF) is only slightly less accurate than a standard page-fault attack.

Effectiveness Against Detection Tools. To analyze the effectiveness of our strategy against detection tools, we measure specificity and recall for different AEX thresholds. We only assume the victim is equipped with the ideal detection tool—as T-SGX supports only C, we could not instrument OpenCV using T-SGX. Figure 15 shows that no threshold value can achieve high specificity and high recall at the same time. In particular, if the detection threshold is smaller than 17, then specificity falls below 0.84 (i.e., a false alarm is raised 2 out of 10 times). At the same time, a detection threshold equal to or bigger than 11 allows attacks to go undetected (recall=0.003). We also note that Our-PF causes no noticeable overhead in terms of cache misses or execution time. We conclude that an ideal detection tool—one that monitors number of AEXs, cache misses or execution time—may not be able to tell an attack that uses our strategy from a benign run of the victim enclave.

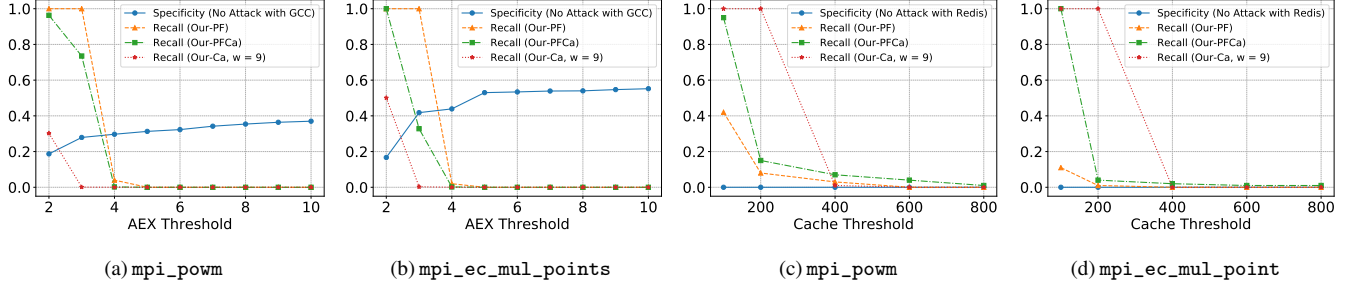


Figure 13: Specificity and recall of detection based on the ideal tool.

		Attack Accuracy	AEX	L3 Cache-misses	Time (ms)
No attack	DTreesImpl::predictTrees		7.83 ($\sigma=0.49$)	134.55 ($\sigma=85.38$)	2.46 ($\sigma=0.06$)
	DTreesImpl::predictTrees (w/GCC)		16.74 ($\sigma=1.44$)	132.42 ($\sigma=73.18$)	2.55 ($\sigma=0.03$)
Standard attack	Page-faults attack	65.2 ($\sigma=0$)	3070.9 ($\sigma=1.4$)	2164 ($\sigma=5455.22$)	58.81 ($\sigma=0.41$)
Our attack	Our-PF	54.9% ($\sigma=3.61\%$)	8.21 ($\sigma=1.34$)	150.77 ($\sigma=74.67$)	2.47 ($\sigma=0.08$)

Table 5: Accuracy and performance metrics for DTreesImpl::predictTrees with an ideal detection tool.

```

1 float DTreesImpl::predictTrees( const Range& range,
2   const Mat& sample, int flags ) const
3 {
4   /* init */
5   for( int ridx = range.start; ridx < range.end; ridx++ )
6   {
7     /* traverse from roots */
8     int nidx = roots[ridx], prev = nidx, c = 0;
9
10    for(;;)
11    {
12      prev = nidx;
13      const Node& node = nodes[nidx];
14      /* reach a leaf node */
15      if( node.split < 0 )
16        break;
17      const Split& split = splits[node.split];
18      int vi = split.varIdx;
19      int ci = cvidx ? cvidx[vi] : vi;
20      float val = psample[ci*sstep];
21      /* update nidx using vi, ci and val */
22    }
23    /* post prediction */
24  }
25 }

```

Figure 14: DTreesImpl::predictTrees used in OpenCV.

7 Concluding Remarks

Our findings show that an adversary can bypass existing tools that monitor performance metrics to detect side-channel attacks on SGX enclaves, by exfiltrating small portions of a secret at each run of the victim. This is particularly relevant for existing cloud-based deployments where enclaves can be restated multiple times by the cloud operator/administrator.

One possible countermeasure would be to tune existing detection tools in order to spot an adversary that uses our strategy. In particular, the tools could keep *state* to detect a pattern of small anomalies spread across multiple executions.

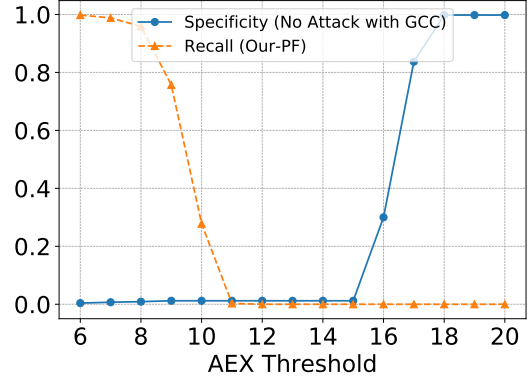


Figure 15: Specificity and recall of detection based on the number of AEXs when GCC is running on the same host.

Intel SGX, however, does not provide freshness of state information sealed to disk. A malicious OS can, therefore, bypass such a tool by providing stale state to the enclave.

Another countermeasure could be to prevent arbitrary restarts of the victim enclave. Namely, the victim enclave may be allowed to execute only upon receiving an authenticated request from, e.g., an authorized user. This is a workable option only if the enclave is used by few users (e.g., in a scenario where a user outsources expensive computations to his enclave deployed in the cloud). Nevertheless, this option is not workable when the enclave provides a “public” service. For example, if the enclave hosts a TLS server [6] or a password-hardening service [16], it is challenging to differentiate between an authorized request from a honest user and another issued by the adversary acting as a honest user.

References

- [1] 97% on MNIST with a single decision tree (+ t-sne). <https://www.kaggle.com/carlolepelaars/97-on-mnist-with-a-single-decision-tree-t-sne>.
- [2] Mnist dataset. <http://yann.lecun.com/exdb/mnist/>.
- [3] Opencv. <https://github.com/opencv/opencv>.
- [4] Redis benchmark. <https://redis.io/topics/benchmarks>.
- [5] Adil Ahmad, Byunggill Joe, Yuan Xiao, Yinqian Zhang, Insik Shin, and Byoungyoung Lee. Obfuscuro: A commodity obfuscation engine on intel sgx. In *NDSS*, 2019.
- [6] Pierre-Louis Aublin, Florian Kelbert, Dan O’Keeffe, Divya Muthukumaran, Christian Priebe, Joshua Lind, Robert Krahn, Christof Fetzer, David M. Eysers, and Peter R. Pietzuch. Libseal: revealing service integrity violations using trusted execution. In *Proceedings of the Thirteenth EuroSys Conference, EuroSys*, pages 24:1–24:15, 2018.
- [7] Maurice Bailleu, Donald Dragoti, Pramod Bhatotia, and Christof Fetzer. Tee-perf: A profiler for trusted execution environments. In *2019 49th Annual IEEE/IFIP International Conference on Dependable Systems and Networks (DSN)*, pages 414–421. IEEE, 2019.
- [8] Ferdinand Brasser, Srdjan Capkun, Alexandra Dmitrienko, Tommaso Frassetto, Kari Kostinen, and Ahmad-Reza Sadeghi. Dr.sgx: Automated and adjustable side-channel protection for sgx using data location randomization. In *Proceedings of the 35th Annual Computer Security Applications Conference, ACSAC ’19*, pages 788–800, New York, NY, USA, 2019. ACM.
- [9] Ferdinand Brasser, Urs Müller, Alexandra Dmitrienko, Kari Kostinen, Srdjan Capkun, and Ahmad-Reza Sadeghi. Software grand exposure: SGX cache attacks are practical. In *USENIX Workshop on Offensive Technologies (WOOT)*, pages 1–12, 2017.
- [10] Samira Briongos, Gorka Irazoqui, Pedro Malagón, and Thomas Eisenbarth. Cacheshield: Detecting cache attacks through self-observation. In Ziming Zhao, Gail-Joon Ahn, Ram Krishnan, and Gabriel Ghinita, editors, *Proceedings of the Eighth ACM Conference on Data and Application Security and Privacy, CODASPY 2018, Tempe, AZ, USA, March 19-21, 2018*, pages 224–235. ACM, 2018.
- [11] Jo Van Bulck, Nico Weichbrodt, Rüdiger Kapitza, Frank Piessens, and Raoul Strackx. Telling your secrets without page faults: Stealthy page table-based attacks on enclaved execution. In *26th USENIX Security Symposium (USENIX Security 17)*, pages 1041–1056, Vancouver, BC, August 2017. USENIX Association.
- [12] G. Chen, W. Wang, T. Chen, S. Chen, Y. Zhang, X. Wang, T. Lai, and D. Lin. Racing in hyperspace: Closing hyper-threading side channels on sgx with contrived data races. In *2018 IEEE Symposium on Security and Privacy (SP)*, pages 178–194, May 2018.
- [13] Sanchuan Chen, Xiaokuan Zhang, Michael K. Reiter, and Yinqian Zhang. Detecting privileged side-channel attacks in shielded execution with déjà vu. In *ACM Asia Conference on Computer and Communications Security, (AsiaCCS)*, pages 7–18, 2017.
- [14] Daniel Gruss, Julian Lettner, Felix Schuster, Olya Ohrimenko, Istvan Haller, and Manuel Costa. Strong and efficient cache side-channel protection using hardware transactional memory. In *26th USENIX Security Symposium (USENIX Security 17)*, pages 217–233, Vancouver, BC, August 2017. USENIX Association.
- [15] Daniel Gruss, Clémentine Maurice, Klaus Wagner, and Stefan Mangard. Flush+ flush: a fast and stealthy cache attack. In *International Conference on Detection of Intrusions and Malware, and Vulnerability Assessment*, pages 279–299. Springer, 2016.
- [16] Arseny Kurnikov, Klaudia Krawiecka, Andrew Paverd, Mohammad Mannan, and N. Asokan. Using safekeeper to protect web passwords. In *The Web Conference, WWW*, pages 159–162, 2018.
- [17] Fangfei Liu, Yuval Yarom, Qian Ge, Gernot Heiser, and Ruby B Lee. Last-level cache side-channel attacks are practical. In *2015 IEEE symposium on security and privacy*, pages 605–622. IEEE, 2015.
- [18] Clémentine Maurice, Nicolas Le Scouarnec, Christoph Neumann, Olivier Heen, and Aurélien Francillon. Reverse engineering intel last-level cache complex addressing using performance counters. In *International Symposium on Recent Advances in Intrusion Detection*, pages 48–65. Springer, 2015.
- [19] Ahmad Moghimi, Gorka Irazoqui, and Thomas Eisenbarth. Cachezoom: How SGX amplifies the power of cache attacks. In *International Conference on Cryptographic Hardware and Embedded Systems (CHES)*, pages 69–90, 2017.
- [20] Olga Ohrimenko, Felix Schuster, Cédric Fournet, Aastha Mehta, Sebastian Nowozin, Kapil Vaswani, and Manuel

- Costa. Oblivious multi-party machine learning on trusted processors. In *25th USENIX Security Symposium (USENIX Security 16)*, pages 619–636, 2016.
- [21] Oleksii Oleksenko, Bohdan Trach, Robert Krahn, Mark Silberstein, and Christof Fetzer. Varys: Protecting SGX enclaves from practical side-channel attacks. In *USENIX Annual Technical Conference (ATC)*, pages 227–240, 2018.
- [22] Meni Orenbach, Yan Michalevsky, Christof Fetzer, and Mark Silberstein. Cosmix: A compiler-based system for secure memory instrumentation and execution in enclaves. In *2019 USENIX Annual Technical Conference (USENIX ATC 19)*, pages 555–570, Renton, WA, July 2019. USENIX Association.
- [23] Michael Schwarz, Samuel Weiser, Daniel Gruss, Cl  mentine Maurice, and Stefan Mangard. Malware guard extension: Using SGX to conceal cache attacks. In *International Conference on Detection of Intrusions and Malware, and Vulnerability Assessment - 14th International Conference (DIMVA)*, pages 3–24, 2017.
- [24] Ming-Wei Shih, Sangho Lee, Taesoo Kim, and Marcus Peinado. T-sgx: Eradicating controlled-channel attacks against enclave programs. In *Network and Distributed System Security Symposium 2017 (NDSS’17)*. Internet Society, February 2017.
- [25] Shweta Shinde, Zheng Leong Chua, Viswesh Narayanan, and Prateek Saxena. Preventing page faults from telling your secrets. In *ACM Asia Conference on Computer and Communications (AsiaCCS)*, pages 317–328, 2016.
- [26] Shweta Shinde, Dat Le Tien, Shruti Tople, and Prateek Saxena. Panoply: Low-tcb linux applications with sgx enclaves. In *NDSS*, 2017.
- [27] O Sury and R Edmonds. Edwards-curve digital security algorithm (eddsa) for dnssec. Technical report, RFC 8080 (Proposed Standard). Internet Engineering Task Force, 2017.
- [28] Jo Van Bulck, Frank Piessens, and Raoul Strackx. Sgx-step: A practical attack framework for precise enclave execution control. In *Proceedings of the 2nd Workshop on System Software for Trusted Execution*, pages 1–6, 2017.
- [29] Jo Van Bulck, Frank Piessens, and Raoul Strackx. Nemesis: Studying microarchitectural timing leaks in rudimentary cpu interrupt logic. In *Proceedings of the 2018 ACM SIGSAC Conference on Computer and Communications Security, CCS ’18*, page 178–195, New York, NY, USA, 2018. Association for Computing Machinery.
- [30] Wenhao Wang, Guoxing Chen, Xiaorui Pan, Yinqian Zhang, XiaoFeng Wang, Vincent Bindschaedler, Haixu Tang, and Carl A. Gunter. Leaky cauldron on the dark land: Understanding memory side-channel hazards in SGX. In *ACM SIGSAC Conference on Computer and Communications Security (CCS)*, pages 2421–2434, 2017.
- [31] Ofir Weisse, Valeria Bertacco, and Todd Austin. Regaining lost cycles with hotcalls: A fast interface for sgx secure enclaves. *ACM SIGARCH Computer Architecture News*, 45(2):81–93, 2017.
- [32] Yuanzhong Xu, Weidong Cui, and Marcus Peinado. Controlled-channel attacks: Deterministic side channels for untrusted operating systems. In *IEEE Symposium on Security and Privacy (SP)*, pages 640–656, 2015.
- [33] Yuval Yarom and Katrina Falkner. Flush+ reload: a high resolution, low noise, l3 cache side-channel attack. In *23rd USENIX Security Symposium (USENIX Security 2014)*, pages 719–732, 2014.